COMPARISON OF MECHANICAL AND ELECTRICAL PROPERTIES OF PIEZOELECTRIC COMPOSITES PZT/ZnO AND PZT/Al_2O_3 FABRICATED BY POWDER METALLURGY

M. Khaleghian, M. Kalantar* and S. S. Ghasemi

* *mkalantar@yazd.ac.ir*

Received: October 2014 **Accepted: April 2015**

Faculty of Mining and Metallurgy, Yazd University, Yazd, Iran.

Abstract: *Lead zirconate titanate (PZT) as a piezoelectric ceramic has been used widely in the fields of electronics, biomedical engineering, mechatronics and thermoelectric. Although, the electrical properties of PZT ceramics is a major considerable, but the mechanical properties such as fracture strength and toughness should be improved for many applications. In this study, lead monoxide, zirconium dioxide and titanium dioxide were used to synthesize PZT compound with chemical formula $Pb(Zr_{0.52},Ti_{0.48})O_3$ by calcination heat treatment. Planetary mill with zirconia balls were used for homogenization of materials. Two-stage calcination was performed at temperatures of 600˚C and 850˚C for holding time of 2h. In order to improve the mechanical properties of PZT, various amount of ZnO and/or Al_2O_3 particles were added to calcined materials and so PZT/ZnO, PZT/Al_2O_3 and PZT/ZnO+Al_2O_3 composites were fabricated. Composites samples were sintered at 1100˚C for 2 h in the normal atmosphere. Microstructural component and phase composition were analyzed by XRD and SEM. The density, fracture strength, toughness and hardness were measured by Archimedes method, three-point bending, direct measurement length crack and Vickers method, respectively. Dielectric and piezoelectric properties of the samples were also measured by LCR meter and d33metet tester, respectively. The results showed that by addition of ZnO and Al_2O_3 to composite materials, the relative density of PZT based composites was increased in conjunction with a signification improvement of mechanical properties such as flexural strength, toughness and hardness. Moreover, the dielectric and piezoelectric properties of PZT such as dielectric constant, piezoelectric coefficient and coupling factor were decreased while the loss tangent was also increased.*

Keywords: *Al_2O_3+ZnO/PZT composites, powder metallurgy, mechanical properties, phase composition, microstructure.*

1. INTRODUCTION

Lead zirconate titanate ceramics (PZT) due to their superior piezoelectric and ferroelectric properties have been used in numerous applications such as electronics, biomedical engineering, thermoelectric, mechatronics, ultrasonic generators, high frequency vibrators [1], activator [2], actuators sensors [3], capacitors aggravating, micro-electromechanical systems (MEMS) [4] and energy converters [5]. For compositions close to the morphotropic boundary phase (MBP) where the proportion of $PbZrO_3$: PbTiO3 is approximately 1:1, piezoelectric and dielectric properties have been significantly improved [6]. Although the electrical properties of PZT ceramics are good, but the mechanical properties such as fracture strength [7] and toughness are relatively poor for many applications [8]. To increase the mechanical properties while maintaining the electrical properties of PZT ceramics, different PZT based composites with second phase as a reinforcing phase such as ZnO [9], Ag [10], Pt [11], MgO [12], ZrO_2 [12] and cement [13] have been developed. For the composites of PZT/Ag and PZT/Pt, the improvement of mechanical properties is much more significant key properties, while the reduction of electrical properties is not much considerable. However, the use of these elements is related to the higher cost and weight of the composites. In this work, the effect of ZnO and Al_2O_3 as a secondary phase on sinterability, microstructural features, mechanical and electrical properties of PZT have been studied.

[DOI: 10.22068/ijmse.12.2.71]

2. MATERIALS AND EXPERIMENTAL METHODS

Monolithic ceramic of PZT and PZT/Al_2O_3 composites were prepared by a simple solid-state mixed oxide method. The starting powders of PbO (99.9%), ZrO_2 (99%) and TiO_2 (99%) were mixed in isopropanol using zirconia balls as a grinding media. Three oxides were mixed with ratios presented in Table 1 in order to obtain a compound with formulation of $Pb(Zr_{0.52}Ti_{0.48})O_3$.

The obtained slurry was dried for 4 hours at 100 °C. To evaluate the optimum temperature for heat treatment of calcination, differential thermal analysis (DTA) and thermal gravity (TG) tests are used in the condition of 1200 °C, argon atmosphere and the heating rate of 10 °C/min on powder mixture of PbO, TiO_2 and ZrO_2 (BAHR-Model STA 504). The homogenized powder was calcined at 600 °C/2h and 850 °C/2h with a heating rate of 1°C/min. The calcined PZT powders were mixed with ZnO or Al_2O_3 and 2%wt PVA as a binder and ball milled in isopropanol for 24 h.

he slurry was then dried and sieved to a fine powder. The mixed powders were uniaxially pressed into pellets at a pressure of 200 MPa. The pellets were sintered in an alumina crucible at 1200 °C for 2h with a heating rate of 10 °C/min. A protecting layer of $PbZrO_3$ powder was applied to minimize PbO evaporation during sintering. However, an additional amount of approximately 0.2% lead oxide in primary mixture was considered. Density, linear shrinkage and phase composition were determined by Archimedes method, comparison dimensions of the sample before and after sintering and X-ray diffraction (XRD), respectively. In order to microscopic observations by scanning electron microscopy (SEM), the sintered samples were polished and were etched in a chemical solution of 95% water and 5% mixture of 95%HCl and 5%HF solution. Fracture strength was carried out by three-point bending method (0.5 mm/min, 4mm × 4mm × 40mm). Fracture toughness was calculated by using direct measurements of the length of crack induced by Vickers indenter [14]:

$$K_{IC} = 0.018\left(\frac{E}{H_V}\right)^{0.4} H_V a^{0.5}\left(\frac{l}{a}\right)^{-0.5} \left(MPa\sqrt{m}\right) \quad (1)$$

Where E is Young's modulus, H_v is Vickers hardness, a is the half length of indentation, and L is the length of crack. The Young's modulus E_{com} was obtained by using the mixture law:

$$E_{com}=E_{PZT}(1-x\%)+E_f x\%, \quad (2)$$

E_{PZT}= 80 GPa, E_f is modulus of reinforcing phase, and x was the volume fraction of reinforcing phase. At least three specimens were used for each measurement of density, hardness, fracture strength and toughness. For electrical measurement, both sides of the sintered pellets were polished, painted with silver paste and fired at 800 °C for 10 min. Prior to measurement of the piezoelectric constant by d33 meter tester, poling treatment was carried out in silicon oil at 20 °C for 20 min with an electric field of 3–4 kV/mm.

Table 1. The percentage by weight and volume fraction of raw materials for the composition of $Pb(Zr_{0.52}Ti_{0.48})O_3$

Type of oxides	Molecular mass (gr/mole)	Weight percent (%)	Volume percent (%)
PbO	223.2	68.55	53.52
TiO_2	79.866	11.77	20.7
ZrO_2	123.218	19.69	25.78

[DOI: 10.22068/ijmse.12.2.71]

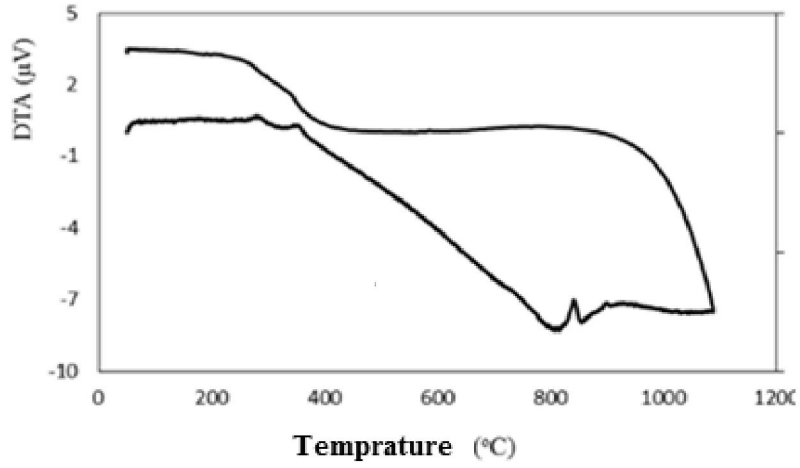

a

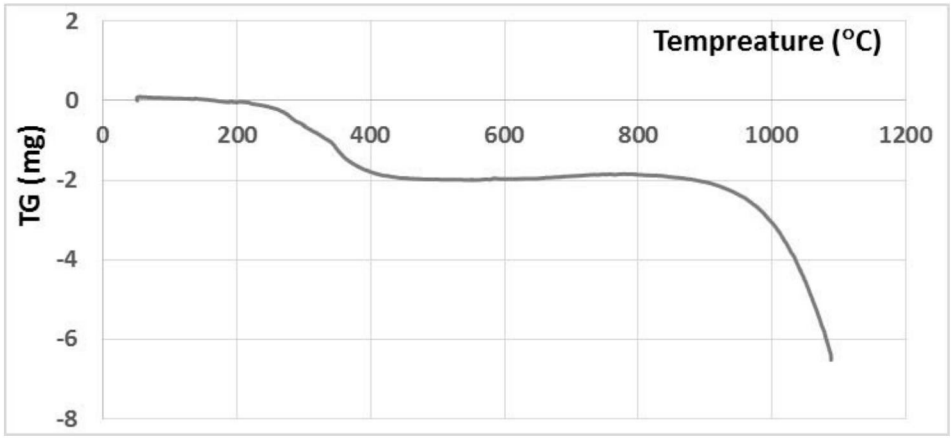

b

Fig. 1. The variation of a: DTA b: TG curves obtained from the mixture of PbO, TiO_2 and ZrO_2 powders ball-milled for 1h.

3. RESULTS AND DISCUSSION

3.1. DTA and TG

According to the DTA analysis results presented in Fig. 1 for mixture powders of PbO, TiO_2 and ZrO_2 ball-milled during 1h, an endothermic reaction has been occurred from 400 to 800 °C that can be related to the formation of PZT. There is an exothermic peak in the temperature of 840 °C corresponding to the crystallization of PZT. Thus, the optimum temperature for the calcination temperature of PZT phase can be 840 - 860 °C. The observation of weight loss from 200 to 400 °C (Fig. 1) can be due to removal of the organic compounds and remaining ethanol. Severe weight loss observed at about 900-1000 °C is corresponding to evaporation of PbO. From the DTA results presented in Fig. 1, it is clear that an endothermic peak has been occurred at around 400 °C, which is related to the exit of organic compounds and burning binder in the sample. PZT phase formation has been occurred at a temperature higher than that of 400 °C because of the endothermic nature of influence.

3.2. XRD Results

The XRD results of calcined samples at 850 °C

[DOI: 10.22068/ijmse.12.2.71]

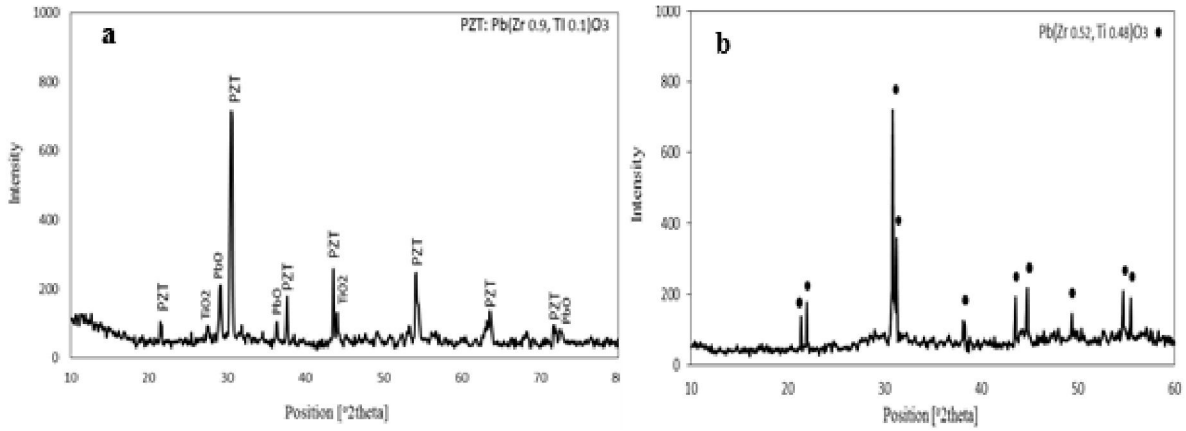

Fig. 2. The XRD patterns taken from the mixture of PZT powders calcined at: (a) 850 °C for 1h; (b) a double-stage of calcination process involving heating at 600 and then 850 °C for 2 hours.

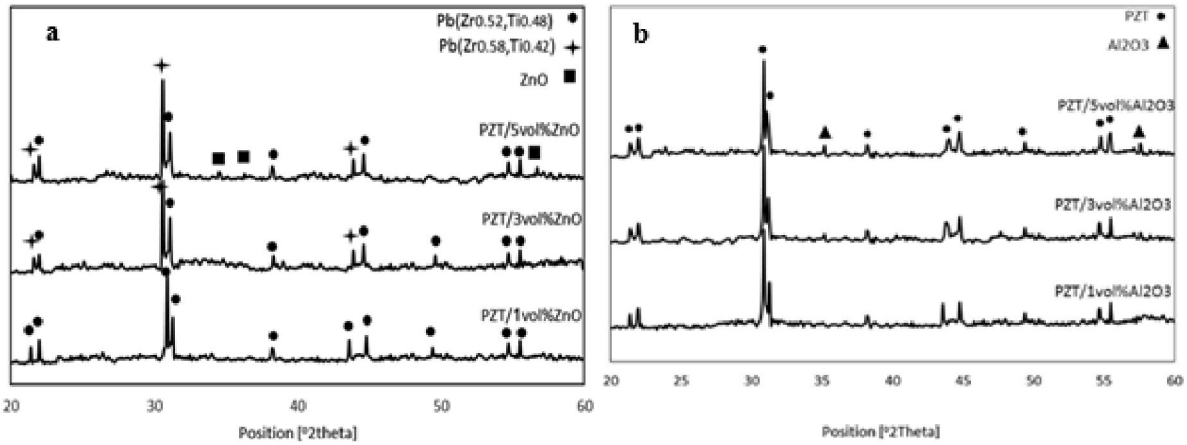

Fig. 3. The XRD patterns of: (a) PZT/ZnO; (b) PZT/ Al_2O_3 composites sintered at 1100 °C/2h.

(Fig. 2(a) show that the phases of PbO and TiO_2 are still in the sample and the composition of PZT is $Pb(Zr_{0.9}Ti_{0.1})O_3$. To achieve the formation of $Pb(Zr_{0.52}Ti_{0.48})O_3$ compound, it has been heat treated under a double stage of calcination process, at first, the powder sample was calcined at 600 °C for 2 hours in order to form $PbTiO_3$ and $PbZrO_3$ and then heated at 850 °C for 2h in order to develop of PZT. The XRD results show that the formation of PZT has been completed by applying the double stage of calcination process (Fig. 2(b)).

According to the XRD patterns given in Fig. 3 for PZT/Al_2O_3 and PZT/ZnO with different percent of ZnO and Al_2O_3 sintered at 1200 °C for 2h, it has been not occurred any chemical reaction between Al_2O_3 and or ZnO with PZT matrix during sintering. With increasing amount of ZnO to the PZT, the compound of PZT has been changed from $Pb(Zr_{0.52}Ti_{0.48})O_3$ with tetragonal structure to $Pb(Zr_{0.58}Ti_{0.42})O_3$ with rhombohedra structure which could be due to the proximity of the atomic radius of Zn with Ti and replacing of Ti ions by Zn ones.

3.3. Physical and Electrical Properties

According to the results shown in Fig. 4, it is clear that the presence of ZnO or Al_2O_3 to the

[DOI: 10.22068/ijmse.12.2.71]

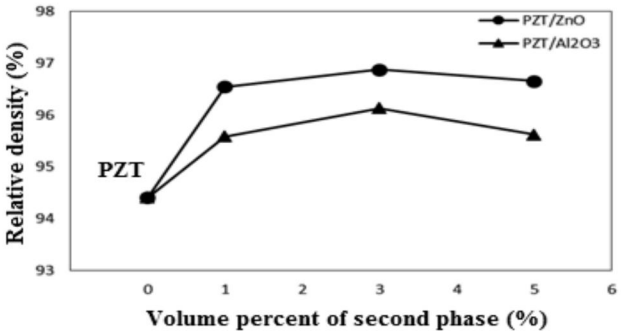

Fig. 4. The effect of ZnO and Al_2O_3 addition on relative density of PZT/ZnO and PZT/Al_2O_3 sintered at 1100 °C/2h.

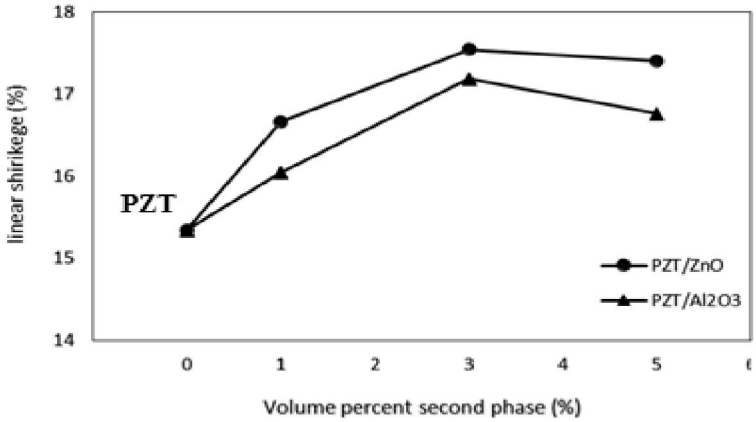

Fig. 5. The effect of ZnO and Al_2O_3 addition on linear shrinkage of PZT/ZnO and PZT/Al_2O_3 sintered at 1100 °C/2h.

PZT has been associated with the higher relative density of the composite in comparison with that of PZT. The maximum values of the relative density are obtained for the PZT/3%ZnO and PZT/3%Al_2O_3 composites which are 96.49 and 96.13%Dth respectively. In fact, by presence of the Zn^{2+} and Al^{3+} ions, the lattice diffusion coefficient is increased by formation of vacancy in PZT and consequently sintering can be more active in the solid state mechanism. On the other hand, the particles of ZnO or Al_2O_3 which are present between the PZT particles can be associated with a significant prevention of grain growth, and therefore, the grain size is considerably reduced. Moreover, the relative density of the PZT/ZnO composite is more than PZT/Al_2O_3, which indicates that ZnO has more effective role than that of Al_2O_3 in the pure PZT. It is interesting to remark that the melting point of ZnO is lower than Al_2O_3 and surface melting of ZnO is greater than Al_2O_3.

For more information, the linear shrinkage of pure PZT, PZT/ZnO and PZT/Al_2O_3 composites are shown in Fig. 5. It can be observed that the liner shrinkage has been increased with the amount of ZnO and Al_2O_3 up to 3Vol%, and then decreases with further increasing of the ZnO and Al_2O_3 to the PZT.

According to the results presented in Figs. 6 to 9, the addition of Al_2O_3 and ZnO particles to PZT, the engineering properties such as dielectric constant (Fig. 6), electromechanical factor (Fig. 7) and piezoelectric load factor (Fig. 8) of PZT are reduced while the dielectric loss tangent (Fig. 9) is increased.

In fact, by presence of ZnO and Al_2O_3 particles to the pure PZT, the grain size of PZT materials has been decreased and therefore the density of

[DOI: 10.22068/ijmse.12.2.71]

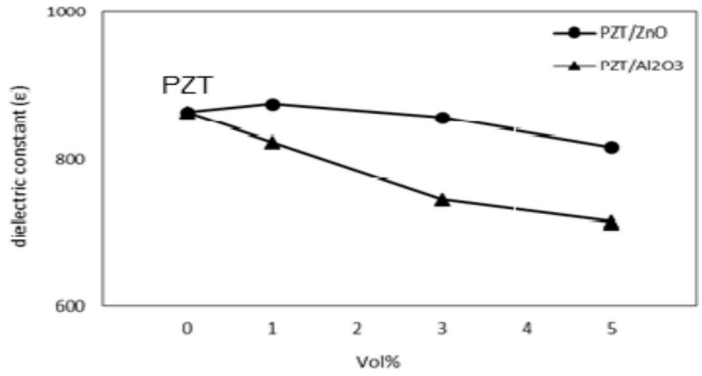

Fig. 6. Diagram of dielectric constant to volume percent (Vol%) of secondary phase for PZT/ZnO and PZT/Al_2O_3 composites.

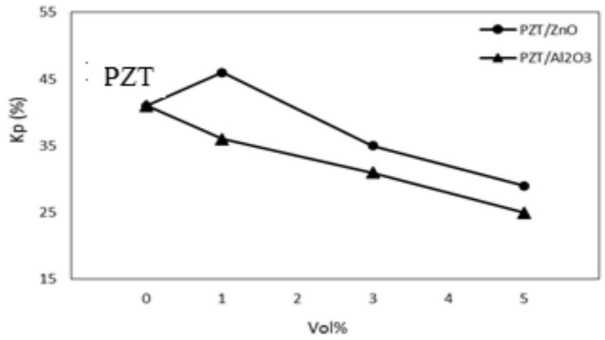

Fig. 7. Diagram of electromechanical factor to volume percent (Vol%) of secondary phase for PZT/ZnO and PZT/Al_2O_3 composites.

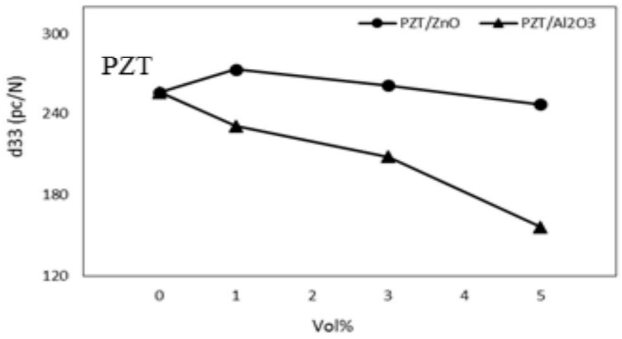

Fig. 8. Diagram of piezoelectric load factor to volume percent (Vol%) of secondary phase for PZT/ZnO and PZT/Al_2O_3 composites.

grain boundary can be increased causing a significant scattering and reduction of electrical properties. On the other hand, Zr^{4+} and Ti^{4+} ions in perovskite lattice can be replaced by Zn^{2+} and Al^{3+} ones which can be resulted to the significant reduction of distance between the centers of positive and negative dipoles and consequently decreasing of piezoelectric properties. Moreover, the dielectric constant, electromechanical factor and piezoelectric load factor are increased slightly for PZT/1vol% ZnO composite. This enhancement can be firstly due to the increasing of relative density and reduction of porosity, and secondly proximity of ionic radio of Zn^{2+} with

[DOI: 10.22068/ijmse.12.2.71]

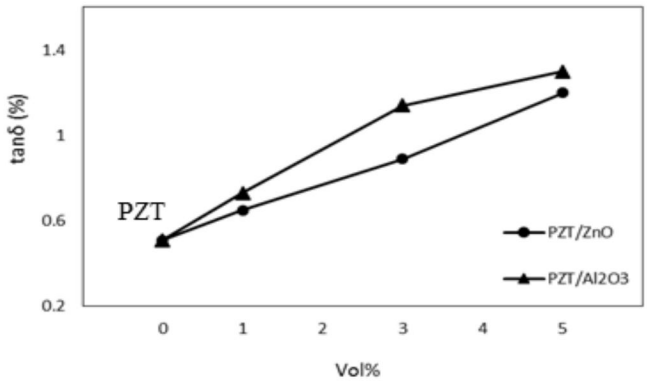

Fig. 9. Diagram of dielectric loss tangent to volume percent (Vol%) of secondary phase for PZT/ZnO and PZT/Al_2O_3 composites.

Ti^{4+} and Zr^{4+}. Replacing of Zr^{4+} or Ti^{4+} by Zn^{2+} has caused a significant level of vacancy in crystalline lattice and therefore increasing of space between center of position and negative dipoles.

3. 4. Microstructural Features and Mechanical Properties

According to SEM micrographs of PZT, PZT/ZnO and PZT/Al_2O_3 samples shown in Fig. 10, the presence of ZnO and Al_2O_3 in PZT as a second phase has resulted to a finer grain microstructure. In fact, the particles of ZnO or Al_2O_3 in grain boundaries of PZT are associated with lowering grain growth during sintering process and so the strength of obtained composites can be higher than that of PZT ceramic (Fig. 11). On the other hand, these particles prevent the formation and propagation of crack in grain boundary areas.

Because of higher hardness and elastic modulus of Al_2O_3 (12 GPa and 375 GPa, respectively) compared to that of ZnO (5 GPa and 210 GPa, respectively), the increasing of strength for PZT/Al_2O_3 composite is more than PZT/ZnO. According to Fig. 12, the hardness for both types of composites are higher than that of PZT monolithic ceramic that can be due to a finer microstructure and higher relative density developed in the composite samples. The higher hardness for PZT/Al_2O_3 composite can be related to the higher hardness of Al_2O_3 particles in comparison with the lower hardness of ZnO. The

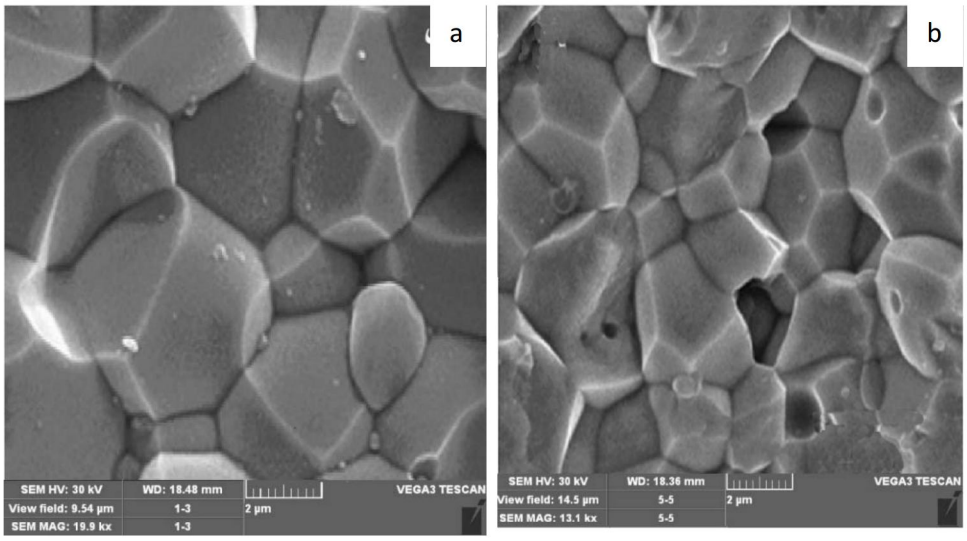

[DOI: 10.22068/ijmse.12.2.71]

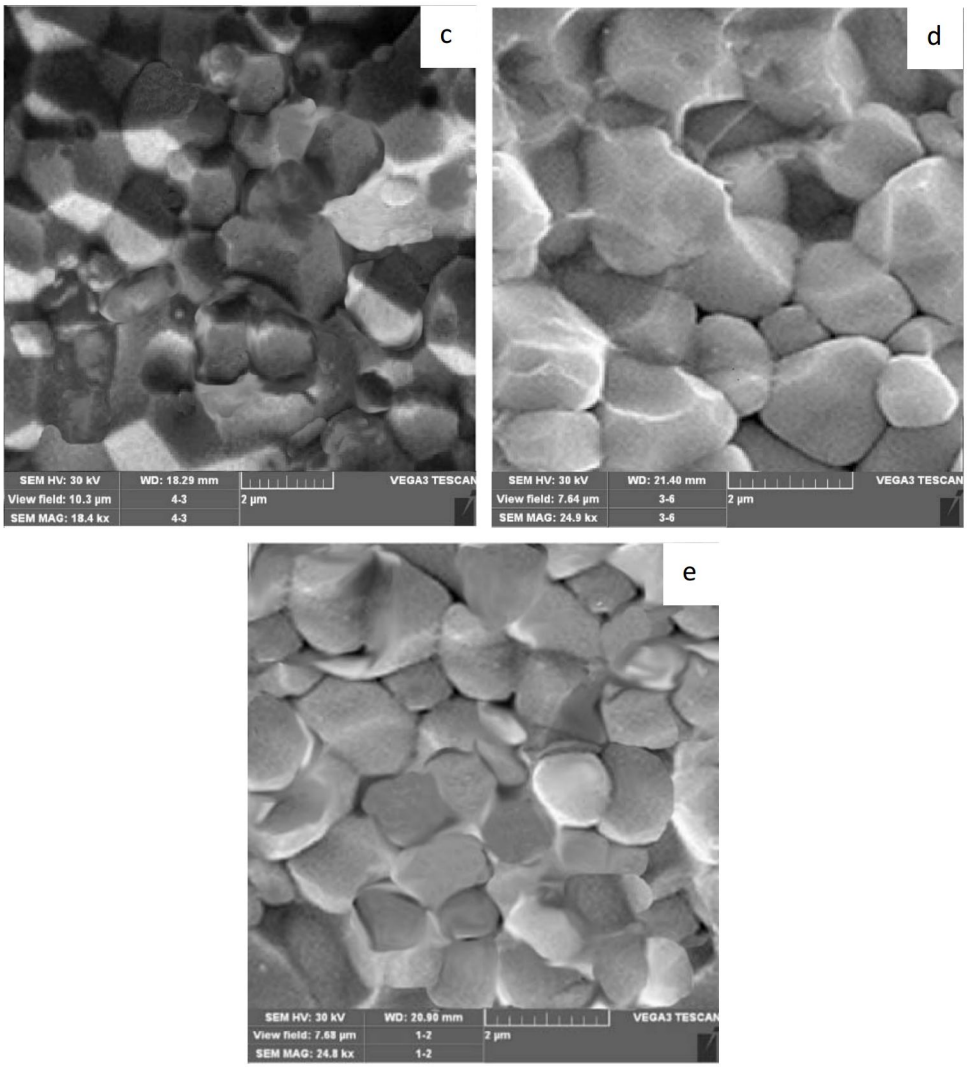

Fig. 10. SEM images of: a) PZT; b) PZT/1Vol%ZnO; c) PZT/3Vol%ZnO; d) PZT/1Vol%Al_2O_3; and e) PZT/3Vol%Al_2O_3.

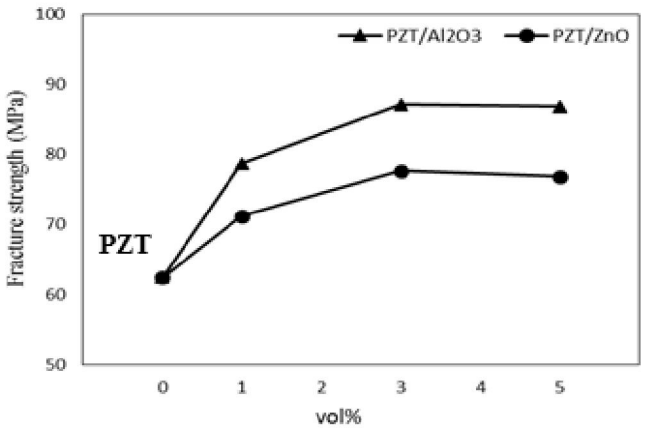

Fig. 11. Bending strength as a function of volume percent (Vol%) of secondary phase for pure PZT, PZT/Al_2O_3 and PZT/ZnO composites.

[DOI: 10.22068/ijmse.12.2.71]

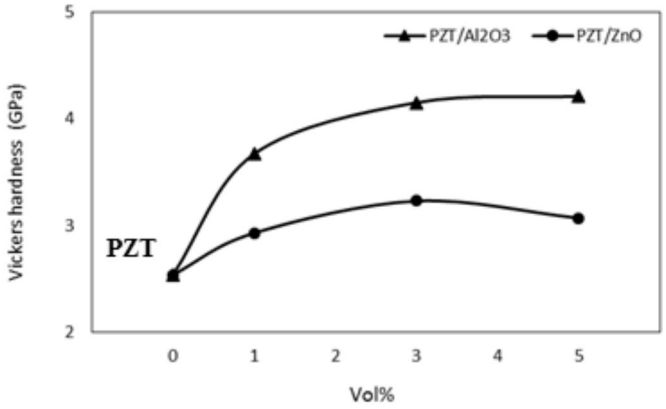

Fig. 12. Vickers hardness as a function of volume percent (Vol%) of secondary phase for pure PZT; PZT/Al_2O_3 and PZT/ZnO composites.

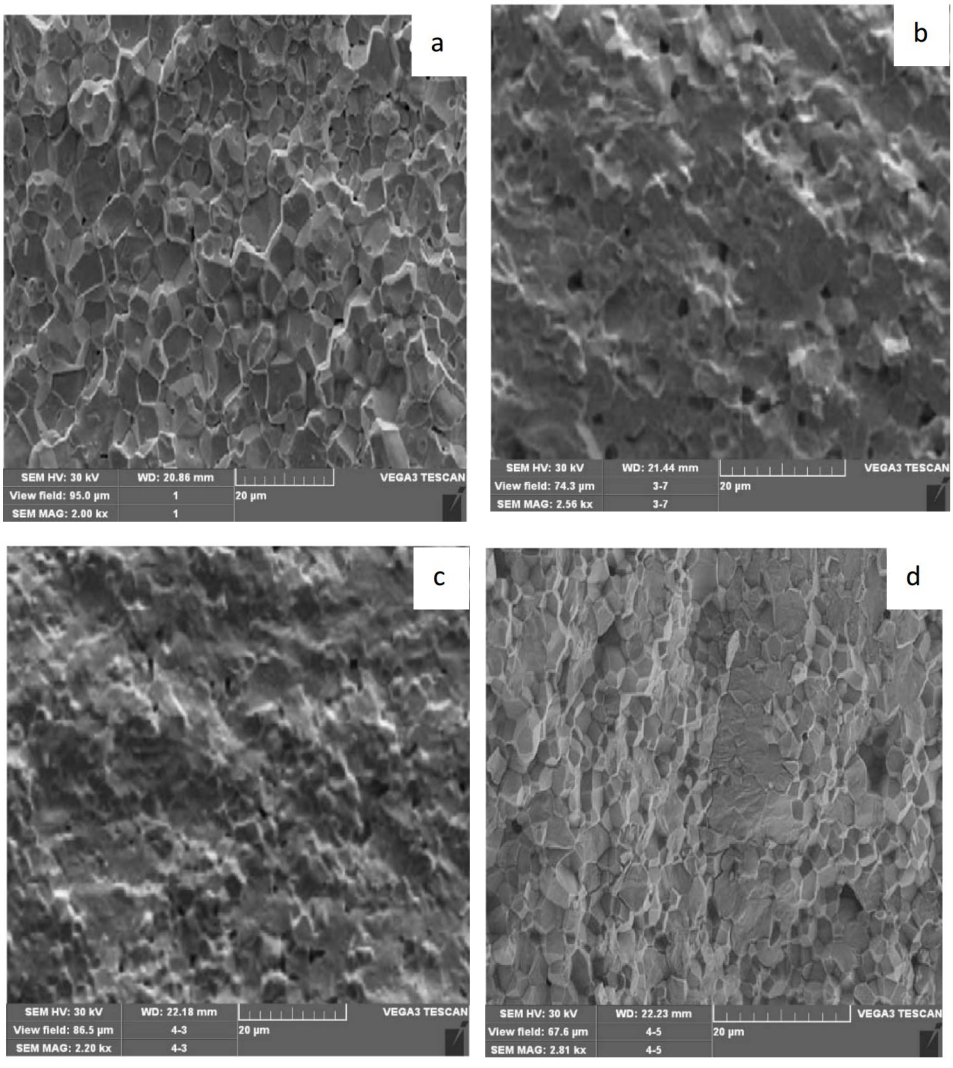

[DOI: 10.22068/ijmse.12.2.71]

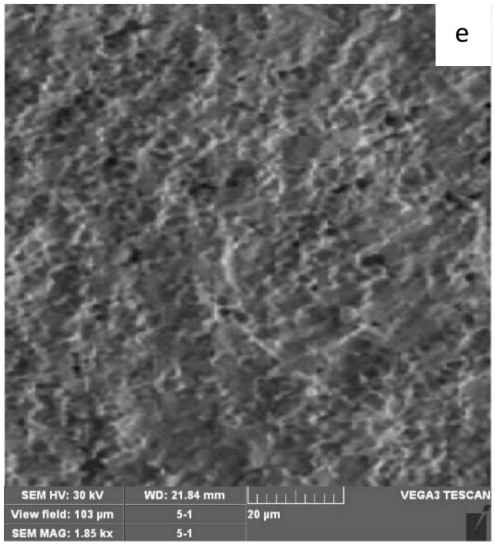

Fig. 13. SEM images of fracture surfaces: a) PZT; b) PZT/1Vol%ZnO; c) PZT/3Vol%ZnO; d) PZT/1Vol%Al_2O_3; and e) PZT/3Vol%Al_2O_3.

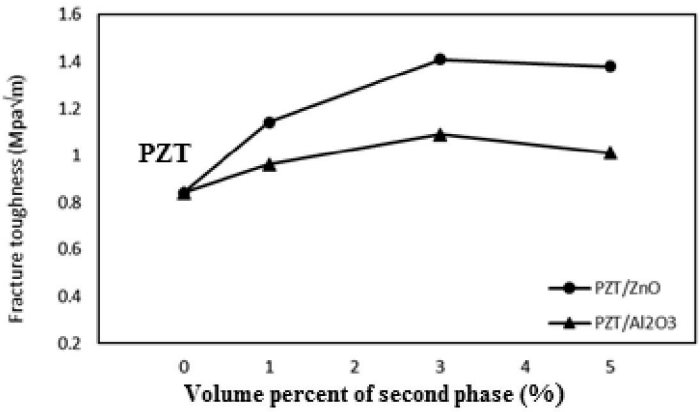

Fig. 14. Fracture toughness as a function of volume percent (Vol%) of secondary phase for PZT/ZnO and PZT/Al_2O_3 composites.

most hardening increasing have been occurred for PZT/5Vol%Al_2O_3 and PZT/3Vol%ZnO composite samples which have been associated with the higher hardness of 66% and 27%, respectively in comparison with that of PZT hardness value.

According to the SEM micrographs of fracture surfaces of PZT, PZT/ZnO and PZT/Al_2O_3 samples shown in Fig. 13, the dominate mechanism of fracture for PZT sample is intergranular. However, the fracture surfaces of the PZT/ZnO and PZT/Al_2O_3 composite samples are rougher than that of the monolithic ones and that the roughness of fracture surfaces has been increased with increasing of ZnO and Al_2O_3 content. In other words, the fracture behavior of PZT/ZnO and PZT/Al_2O_3 composites is a mixture of transgranular and intergranular modes.

In fact, by presence of ZnO or Al_2O_3 particles in the pure PZT, the strength of grain boundaries has been improved and consequently the percentage of intragranular fracture is not predominate, although the strength and toughness can be simultaneously increased (Figs 11, 14).

According to the light micrographs of Vickers indentation presented in Fig.15, the crack length created on the composite sample surfaces is much

[DOI: 10.22068/ijmse.12.2.71]

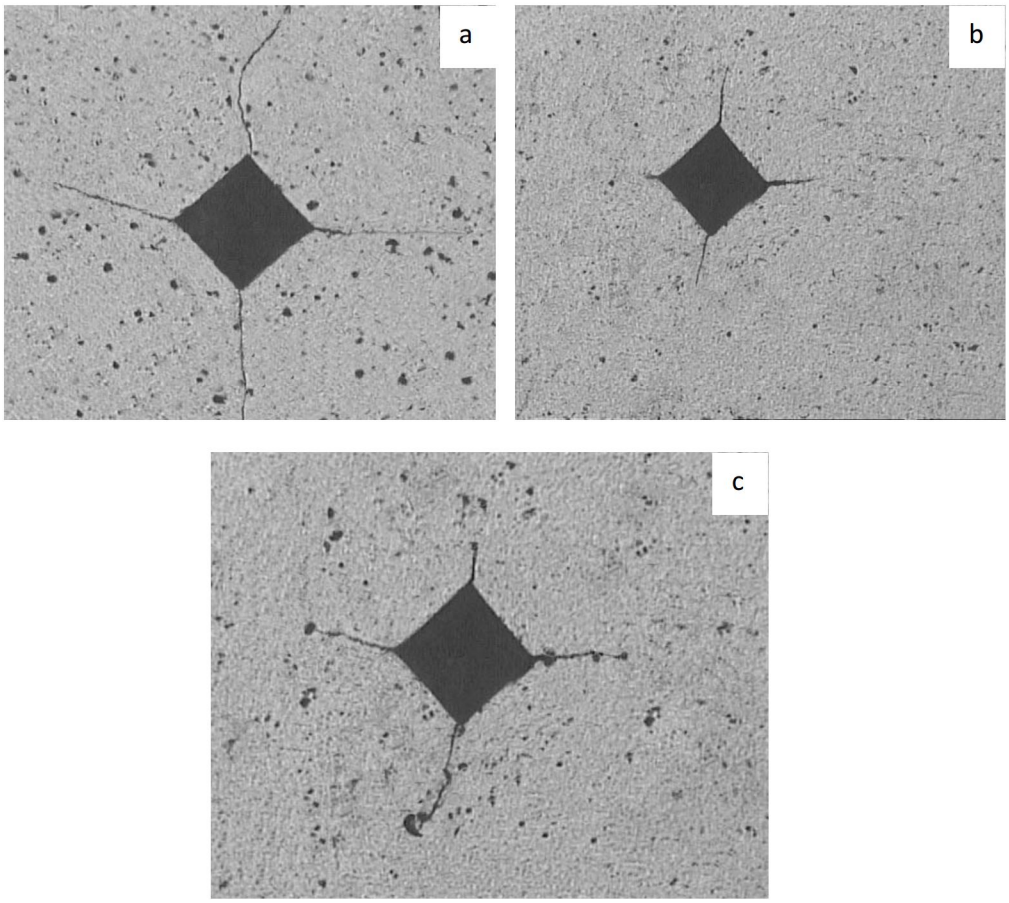

Fig. 15. Optical microscope images of Vickers indentation: a) PZT; b) PZT/3Vol%Al_2O_3; and c) PZT/3Vol%ZnO

less than that of PZT samples indicating a higher resistance to crack growth has been occurred for the composite samples. Moreover, a higher relative density, the higher strength and more resistance to the propagation of crack in grain boundary are associated for the higher toughness of the composite samples. The higher resistance to crack growth in composite samples can be related to the crack bridging developed by Al_2O_3 and ZnO particles, which reduces the energy of crack growth. Moreover, the higher toughness of PZT/ZnO composite samples in comparison with that of PZT/Al_2O_3 samples can be due to the higher density of PZT/ZnO as well.

4. CONCLUSIONS

1. A double stage of calcination involving firstly heated at 600□C and then at 800 °C for 2 hours has been related with a perfect formation of PZT.
2. Al_2O_3 and ZnO particles as a reinforced phase are non-sensitive to chemical reaction with PZT and are compatible with it.
3. By adding of Al_2O_3 and ZnO particles to the PZT ceramic, the sinterability has been increased and the highest relative density is obtained for PZT/3Vol%ZnO and PZT/3Vol%Al_2O_3 samples.
4. By adding of Al_2O_3 and ZnO particles simultaneously to the PZT samples, a finer microstructure has been obtained in comparison to that of pure PZT and PZT based composite samples (Al_2O_3/PZT and ZnO/PZT).
5. Fracture mechanism of PZT samples is intergranular mode while for PZT/ZnO and

[DOI: 10.22068/ijmse.12.2.71]

PZT/Al_2O_3 composites are a combination of intergranular and intragranular modes.

6. By adding of Al_2O_3 and ZnO to the PZT samples, the strength, fracture toughness and hardness are increased. The highest strength and hardness values are obtained for PZT/Al_2O_3 samples in the manner of 85MPa and 4.5 GPa, respectively; while the highest toughness is obtained for PZT/ZnO composite ones (1.4 MPa.m1/2).
7. By adding of Al_2O_3 and ZnO to the PZT samples, the electerical properties such as dielectric constant, piezoelectric load factor and electromechanical factor are slightly reduced while the loss tangent is increased.

REFERENCES

1. Meng, X., Yang, C., Fu, W. and Wan, J., "Preparation and electrical properties of ZnO/PZT films by radio frequency reactive", Materials Letters, 2012, 83 179–182.
2. Sangsubum, C., Naksata, M. and Watcharapasorn, A., "Optimal fabrication and sintering properties of PZT ceramics from sol-gel powder", Department of Physics, Faculty of Science, Chiang Mai university, Chiang Mai 50200, Thailand, 2009.
3. Sangsubun, C., Naksata, M., Watcharapasorn, A., Tunkasiri, T. and Jiansirisomboon, S., "Preparation of PZT Nanopowders via sol-gel Processing", Department of Physics, Faculty of Science, Chiang Mai University, Chiang Mai 5200,Thailand, 2010.
4. Gebhardt, S., Seffner, L., Schlenkrich, F. and Schonecker, A., "PZT thick films for sensor and actuator applications", Journal of the European Ceramic Society, 2007, 27 4177–4180.
5. Dong, W., Lu, X., Cui, Y., Wang, J. and Liu, M., "Fabrication and characterization of microcantilever integrated with PZT thin film sensor and actuator", Thin Solid Films, 2007515 8544–8548.
6. Xiong, S., Kawada, H., Yamanaka, H. and Matsushima, T., "Piezoelectric properties of PZT films prepared by the sol–gel method and their application in MEMS", Thin Solid Films, 2008, 516 5309–5312.
7. Hindrichsen, C. G., Møller, R. L., Hansen, K. and Thomsen, E. V., "Advantages of PZT thick film for MEMS sensors", Sensors and Actuators, 2010, A163 9–14.
8. Wang, D. W., Cao, M. S. and Yuan, J., "Effect of sintering temperature and time on densification, microstructure and properties of the PZT/ZnO nano-whisker piezoelectric composites", Journal of Alloys and Compounds, 2011, 509 6980–6986.
9. Gong, Z. Li, H., Zhang, Y., "Fabrication and piezoelectricity of 0–3 cement based composite with nano-PZT powder", Current Applied Physics, 20099 588–591.
10. Zhang, H. L., Li, J. F., Zhang, B. P. and Jiang, W., "Enhanced mechanical properties in Ag-particle-ispersed PZT piezoelectric composites for actuator applications", Materials Science and Engineering A, 2008, 498 272–277.
11. Li, J. F., Takagi, K., Terakubo, N. and Watanabe, R., "Electrical and mechanical properties of piezoelectric ceramic/metal composites in the $Pb(Zr,Ti)O_3$/Pt system", Appl. Phys. Lett., 2001, 79 (15) 2441–2443.
12. Tajima, K., Hwang, H., Sando, M. and Niihara, K., "PZT nanocomposites reinforced by small amount of oxide", Journal of the European Ceramic Society, 1999, 19 1179–1182.
13. Chaipanich, A., "Effect of PZT particle size on dielectric and piezoelectric properties of PZT–cement composites", Current Applied Physics, 2007, 7 574–577.
14. Niihara, K., Morena, R. and Hasselman, D. P. H., J. Mater. Sci. Lett., "Evaluation of KIc of brittle solids by the indentation method with low crack-to-indent ratios", 1982, 1 13–16.

[DOI: 10.22068/ijmse.12.2.71]